

Fast iterative beam hardening correction based on frequency splitting in computed tomography

Qiao Yang^{a,b}, Matthias Elter^b, Ingo Schasiepen^b, Nicole Maass^b and Joachim Hornegger^{a,c}

^aPattern Recognition Lab, Friedrich-Alexander-University Erlangen-Nuremberg,
Erlangen, Germany

^b Siemens AG, Healthcare Sector, Erlangen, Germany

^c School in Advanced Optical Technologies (SAOT), Erlangen, Germany

ABSTRACT

In computed tomography (CT), the nonlinear characteristics of beam hardening are due to the polychromaticity of X-rays, which severely degrade the CT image quality and diagnostic accuracy. The correction of beam hardening has been an active area since the early years of CT, and various techniques have been developed. State-of-the-art works on multi-material beam hardening correction (BHC) are mainly based on segmenting datasets into different materials, and correcting the non-linearity iteratively. Those techniques are limited in correction effectiveness due to inaccurate segmentation. Furthermore, most of them are computationally intensive. In this study, we introduce a fast BHC scheme based on frequency splitting with the fact that beam hardening artifacts mainly contain in the low frequency components and take more iterations to be corrected in comparison with high frequency components. After low-pass filtering and correcting artifacts at down-sampled projections, an artifact reduced high resolution reconstruction will be obtained by incorporating the original edge information from the high frequency components. Evaluations in terms of correction accuracy and computational efficiency are performed using simulated and real CT datasets. In comparison to the BHC algorithm without frequency splitting, the proposed accelerated algorithm yields comparable results in correcting cupping and streak artifacts with tremendously reduced computational effort. We conclude that the presented framework can achieve a significant speedup while still obtaining excellent artifact reduction. This is a significant practical advantage for clinical as well as industrial CT.

Keywords: Computed tomography, image reconstruction, beam hardening artifacts

1. MOTIVATION

In computed tomography (CT), the polychromatic characteristic of X-rays leads to the attenuation of an homogeneous object being not proportional to the thickness of the object along the ray. When a polychromatic X-ray beam passes through objects, lower energy photons are more easily absorbed than the higher energy photons, resulting in so-called beam hardening phenomenon. Standard reconstruction techniques, such as filtered back-projection (FBP), are generally based on the assumption that the linear attenuation coefficient for a certain object is unique and that the logarithm of the measurement is the line integral of the attenuation coefficient. Therefore, if the energy dependence of the X-ray is not taken into account, reconstruction images will contain cupping and streak artifacts¹.

To mitigate artifacts caused by beam hardening, numerous correction techniques have been proposed. The very first and common approach is to absorb the lower energy photons in the spectrum by physically pre-filtering the X-ray beams with thin metallic plates. Although the hardware filters limit the amount of beam hardening, the narrowed source spectrum with lower photon count also results in a decrease of the signal-to-noise ratio. State-of-the-art BHC approaches used in clinical CT are mainly based on water-equivalent calibration and can only efficiently correct datasets consisting of objects which have similar densities as water. Alvarez² proposed dual-energy correction which is capable to eliminate beam hardening artifacts. However, the major drawback of dual-energy lies in the requirement of sophisticated and expensive hardware calibration. Pre-correction is

Send correspondence to Qiao Yang: qiao.yang@informatik.uni-erlangen.de

generally based on linearization procedures.³ Here, the nonlinear measurement is fitted with polynomials as one assumes that all substances in the scanning plane have the same energy dependence. The post-processing techniques^{4,5} start with a preliminary reconstruction, from which a material distribution is calculated. The distribution allows estimation of the hardening factor, thus the corrected reconstruction can be obtained by correcting the original projection images. Scientific researches for datasets consisting of multiple materials are often carried out by segmenting the datasets into different materials and correcting the non-linearity iteratively. A major limitation of these techniques is computational complexity which renders them unsuitable for practical usage^{5,6,7}.

In this work, we employ the material decomposition approach from dual-energy model into standard single tube energy CT. By acquiring material distribution and density information for segmented volume, a polychromatic model can be obtained from combination of material density. Doing the segmentation that way is essential in order to obtain a high image quality because of the following reasons:

a fast BHC algorithm based on frequency splitting. Frequency splitting techniques have been used in CT for various purposes such as image reconstruction⁸, scatter correction⁹ and metal artifact reduction¹⁰. We employ this technique by low-pass filtering the original images to avoid aliasing during down- and up-sampling, and apply most of the BHC iterations to the down-sampled projection images to reduce the computational intensity.

We organize the paper as follows: section 2 outlines the theoretical aspects of the proposed algorithm. The method has been evaluated for simulated and real X-ray CT data, which can be found in section 3. Finally, discussion and conclusion are presented in section 4.

2. METHODS

In this section, we briefly introduce the framework of the accelerated iterative BHC using frequency splitting. A flowchart of the algorithm can be found in Fig. 1. The algorithm mainly can be divided into two parts: it is initialized by performing frequency splitting on original projection images to obtain low resolution images and an iterative scheme which corrects beam hardening artifacts on down-sampled images. It has to be noted that sampling errors may occur during the procedure, therefore, final refinement of the images has to be taken under consideration.

2.1 Frequency split

The algorithm is based on the observation that beam hardening artifacts mainly appear in the lower frequency components of the image and cause more correction iterations than correction in high frequency components. Correcting beam hardening at down-scaled images will significantly limit the computational time but is still be able to preserve correction quality. A low-pass filter is applied to split the projections I into low frequency components I^{LF} and high frequency components I^{HF} . 2D Gaussian filters are applied with a fixed standard deviation to perform the split

$$I_{u,v} = \frac{1}{2\pi\sigma} \cdot e^{-\frac{u^2+v^2}{2\sigma^2}}. \quad (1)$$

Additional high frequency information would be lost during down-scaling process. Therefore, ideally, a filter which anticipates the frequency characteristics of beam hardening corresponds to the downscaling method could be chosen for better accuracy.

2.2 Segmentation

Generally, when BHC approaches contain a segmentation step to distinguish different materials, the performance of the correction algorithms highly depends on the accuracy of that segmentation. However, the segmentation often suffer from the reconstruction artifacts. In this paper, a global thresholding method is used, but we would like to address that when more sophisticated segmentation strategies are applied, the efficiency of the correction method would be improved because of the decrease in number of iterations. Therefore, the major challenge for the correction is to obtain more precise segmentations, which is expected after the iterative reduction of beam hardening artifacts.

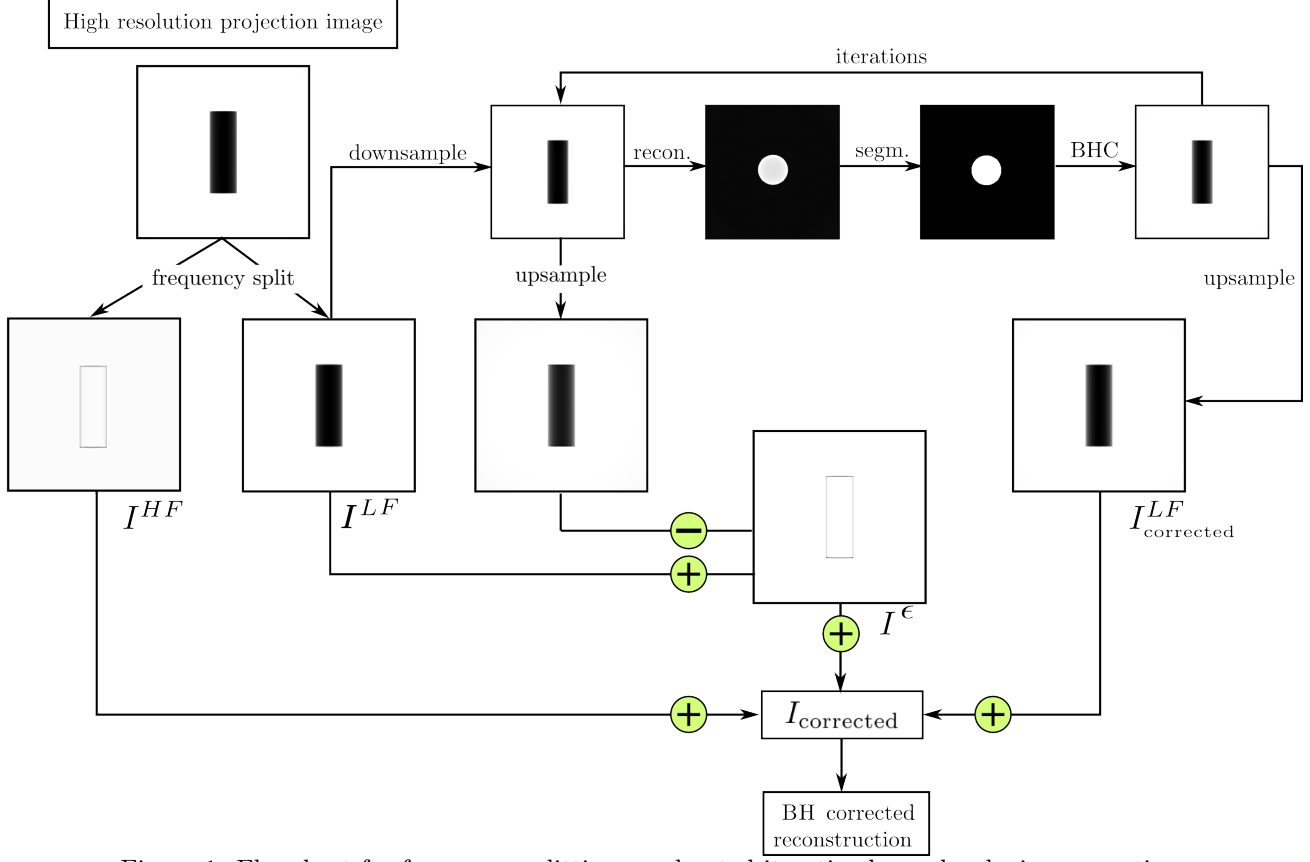


Figure 1: Flowchart for frequency splitting accelerated iterative beam hardening correction.

2.3 Beam hardening correction

When X-ray beams traverse objects, the attenuation coefficients μ are dependent on material characteristics such as mass density ρ , atomic number Z , photon energy E , as well as intersection length s between X-ray beam and objects. According to Lambert-Beer's law, the attenuation of monochromatic X-ray beam i can be modeled as

$$I_{\text{mono},i} = I_0 e^{-\int \mu(\rho, Z, E_0) ds_i}, \quad (2)$$

where I_0 is incident intensity and E_0 is monochromatic photon energy.

However, in practice X-rays are polychromatic, i.e., each photon is part of the polychromatic X-ray spectrum. When energy dependence of the attenuation coefficients $\mu = \mu(\rho, Z, E)$ is taken into account, the exit intensity for the specific beam i can be expressed as

$$I_{\text{poly},i} = \int_0^{E_{\text{max}}} I_0(E) e^{-\int \mu(\rho, Z, E) ds_i} dE, \quad (3)$$

where $I_0(E)$ is the X-ray source spectrum.

In our approach, the aim is to find correction factors α by simulating monochromatic and polychromatic projections

$$\alpha = \frac{I_{\text{mono}}}{I_{\text{poly}}}. \quad (4)$$

With the measured X-ray intensities I_{original} as reference, corrected intensities are calculated as follows:

$$I_{\text{correction}} = \alpha \cdot I_{\text{original}}. \quad (5)$$

The smaller the difference between measured projections and corresponding simulated polychromatic intensity image I_{poly} , the higher accuracy the correction factors have. A more detailed description of this BHC method was published in Yang *et al.*¹¹.

Since the accuracy of segmentation results in the efficiency of correction, gradually improvement for both segmentation and beam hardening reduced reconstruction can be obtained iteratively. To derive a stop criterion for the iterations, we define the polychromatic model error ξ of the i th iteration to be the value of cost function Φ where

$$\Phi = \frac{1}{L} \sum_{l=1}^L (I_{\text{poly},l}^{\text{original}} - I_{\text{poly},l}^{\text{sim}})^2. \quad (6)$$

L is the total number of projection rays. Given a threshold $t \in [0; 1]$, the iteration process will be terminated when

$$t < \frac{\xi^i + \xi^{i-1}}{\xi^{i-2} + \xi^{i-3}}. \quad (7)$$

2.4 Corrected projection and further refinement

The corrected downsampled projections are then upsampled to the original resolution projections. To avoid loss of information, the original high-frequency components I^{HF} and the sampling inaccuracies ϵ due to interpolation need to be taken into account:

$$I_{\text{corrected}} = I^{\text{HF}} + I^\epsilon + I_{\text{corrected}}^{\text{LF}}. \quad (8)$$

The proposed method is based on the assumption that the beam hardening artifacts mainly appear in the low frequency components of the projections, which results in more iterations are needed in low frequency components than in high frequencies. After accelerated BHC iterations at downsampled images to reduce the artifacts in low frequencies, one or two final iterations at full resolution are expected to further improve correction accuracy and image quality. This is to compensate the distortions caused by the susceptibility changes at material edges which appear mainly in high frequency components.

In this paper, two iterations with full resolution are applied for both simulated and real datasets for evaluation.

3. RESULTS AND DISCUSSION

In order to investigate the effectiveness of the proposed algorithm, we applied the correction to both simulated and real data. Detailed setup parameters for each dataset are shown in Table 1.

Table 1: Setup parameters

Parameter	Hip Prosthesis Phantom	Multi-cylinders
Tube voltage	120kVp	150kVp
SOD(source object distance)	750mm	1200mm
SDD(source detector distance)	800mm	1400mm
Detector	512×512	1024×1024
Pixel size	0.4mm	0.4mm
Volume	512×512×512	400×400×600
Voxel size	0.3mm	0.5mm

3.1 Simulation results

The validity of the proposed algorithm is evaluated by using a simulated FORBILD hip prosthesis phantom¹². The correction operations were applied using a downsampling factor of two. Fig. 2 shows the FBP reconstruction of the hip prosthesis phantom, segmentation and the line profiles regarding to cupping and streak artifacts, respectively. We illustrate the results for original (iteration 0), intermediate (iteration 5) and final (iteration 11) iterations. From the reconstruction and corresponding line profiles along the central horizontal and vertical line, it can be observed that both cupping and streak artifacts have been strongly suppressed compared to non-corrected reconstruction.

Due to the inaccuracy of the segmentation, over- and under- correction during iterations occur. For example, in the column of Fig. 2 which shows results from iteration 5, an over-correction of cupping artifacts occurred. This is mainly because misclassification of material will lead to errors in simulating different polychromatic characteristics. However, the results depict that our method is able to recover an accurate reconstruction image with precise segmentation, even though the initial segmentation is poor.

The second row of Fig. 2 demonstrates the segmentation for the datasets which consists of three material classes (soft tissue, bone and metal implants). Clearly, gradual improvement of the segmentation image through successive iterations can be observed. From the results shown above, it can be seen that the initial segmentation suffers from reconstruction artifacts at the beginning. During the reducing of beam hardening artifacts, better segmentations can be obtained.

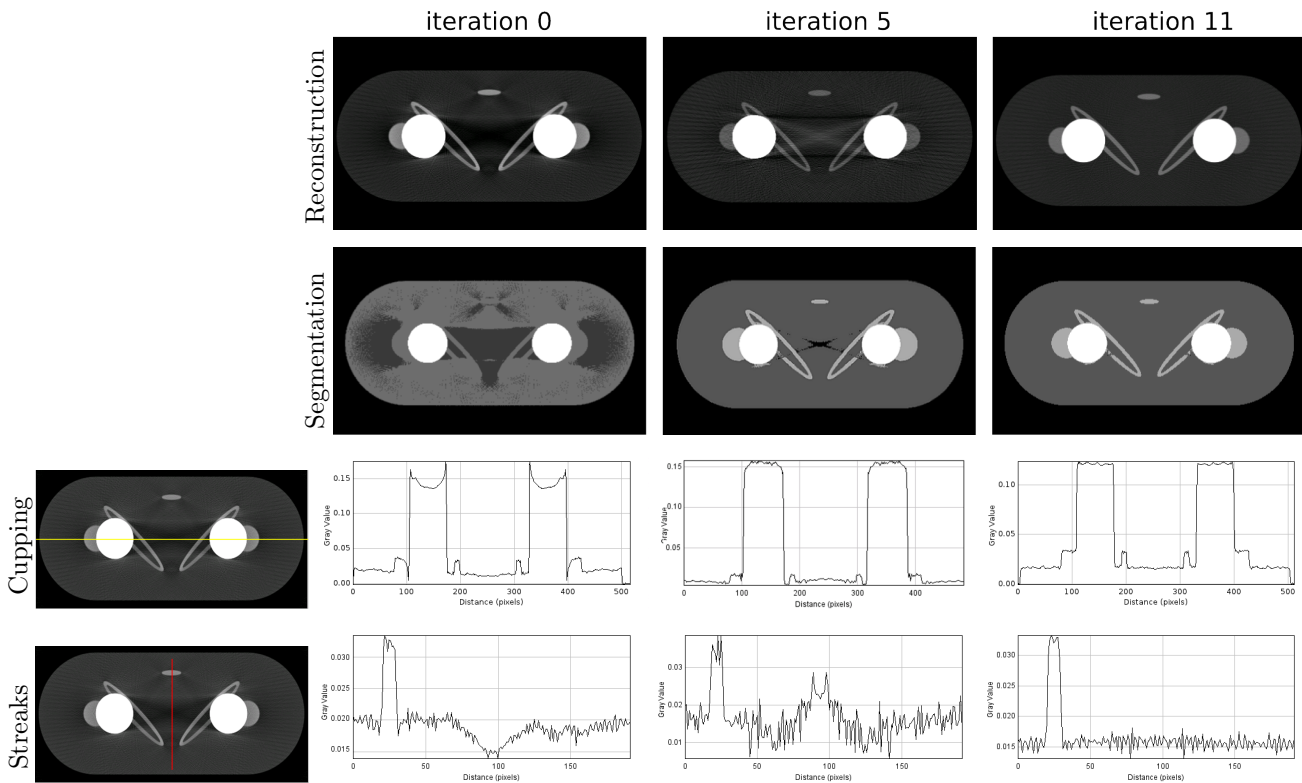


Figure 2: Simulation results from hip prosthesis phantom at original (Iter. 0), intermediate (Iter. 5) and final (Iter. 11) reconstruction, respectively. Iteration 1 to 9 were simulated with a down-sampling factor of 2, and two final iterations were carried out on full resolution images. First row: reconstruction of the phantom. Second row: segmentation. Third row: line profiles along center horizontal line in order to examine cupping artifacts. Bottom row: line profiles along center vertical line in order to examine streak artifacts between two high density prosthesis. Window settings (in terms of attenuation coefficient): level 0.08; window 0.15.

3.2 Experimental results

A real X-ray projected multi-material dataset consisting of four cylinders (polyester, aluminum, steel, and copper) was further evaluated (see Table 1). Figure (3a) shows the central slice of the original reconstruction without BHC and the corresponding line profile. It can be observed that suffering from the existence of high density objects, the original reconstruction shows dark and bright streak artifacts and strong cupping. Moreover, segmentation faces a big challenge due to the similar dense objects which results in overlapping of gray value in histogram and streak distortions.

Fig. (3b) and Fig. (3c) illustrate the reconstruction results from BHC applied on full resolution images and our accelerated algorithm, respectively. The correction with full resolution was carried with 12 iterations with stop criterion $t = 0.78$, while with frequency split method it stopped at 9th iteration with $t = 0.75$. A comparison of our proposed method with the high resolution BHC method indicates that our algorithm is equally effective in removing cupping artifacts. Further examination on reduction of streak artifacts is depicted with the red circle in the line profiles. It can be seen that the BHC algorithm has successfully reduced the streaks caused by beam hardening compared to reconstruction without correction. However, the proposed algorithm is slightly less effective than the BHC applied on full resolution images. The reason might be that part of the streak artifacts appear in the high-frequency components.

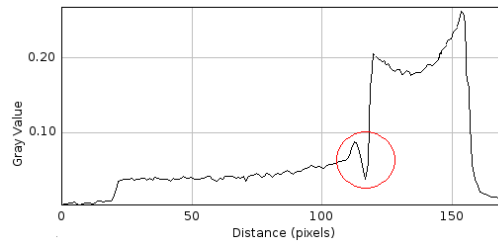
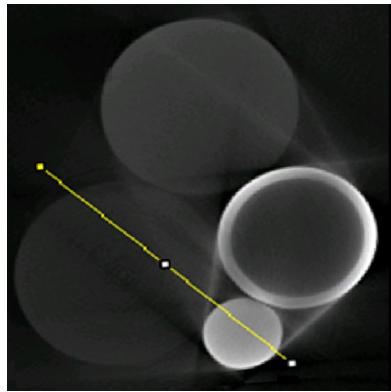
3.3 Computational intensity

The BHC algorithm requires one forward and back projection for each iteration, which significantly hinder the computational speed. By taking most of the iterations at down-scaled images, our method can achieve computationally much less expensive. Theoretically, a down-sampling factor of two yields a reduction of the projection pixel number by factor of four and voxel number by a factor of eight. In our experiments, the running time of simulation dataset was 17.9% of the time cost by BHC with full resolution, and the real dataset achieved 21.2%.

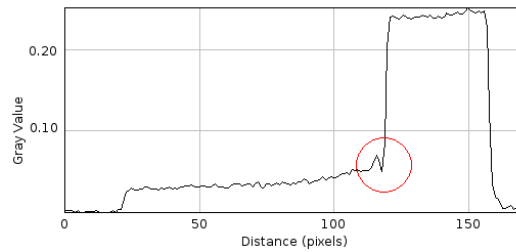
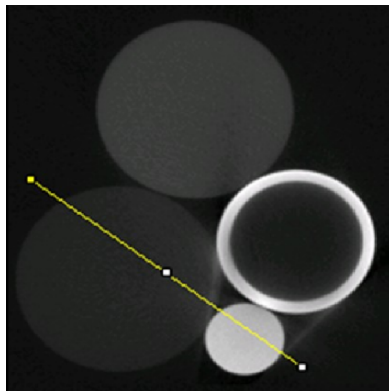
4. CONCLUSION

In this paper, we have presented a fast BHC algorithm based on frequency splitting. The corrected images can be obtained by iteratively correcting down-sampled images with low frequency, and later combining them with the original high-frequency images in order to lower the computation cost. The algorithm has been implemented for a 3D cone beam geometry, which be realized for practical usage.

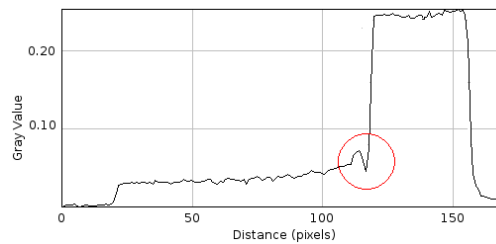
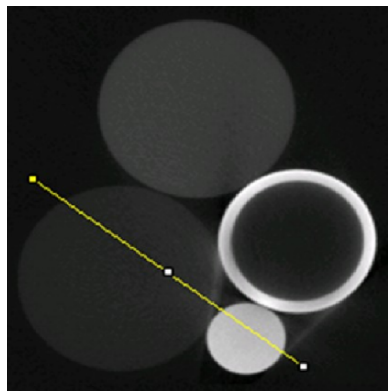
The results presented in this paper indicate that a successful reduction of beam hardening artifacts can be obtained even when the projections have been down-sampled, which proves our initial assumption. In addition, the algorithm has been compared to the full resolution BHC approach and the results yield similar effectiveness for correcting cupping and streak artifacts, but a significant reduction of computational intensity. Using the frequency splitting method enables the general capability of BHC approaches in low resolution images. However, in order to minimize the information loss in the high frequency components, it is necessary to apply full resolution correction at final steps.



(a) Reconstruction without BHC



(b) BHC applied to full resolution images



(c) BHC applied to images after frequency splitting

Figure 3: Reconstruction results of real X-ray projected dataset consisting of copper, steel, aluminum and polyester cylinders, with correspondent line profiles. (3a): slice of original reconstruction without BHC. (3b): slice of reconstruction with BHC in high resolution. (3c): slice of reconstruction with proposed frequency splitting BHC algorithm. Window settings (in terms of attenuation coefficient): level 0.11; window 0.3.

REFERENCES

- [1] Stonestrom, J. P., Alvarez, R. E., and Macovski, A., "A framework for spectral artifact corrections in x-ray CT," *IEEE Transactions on Biomedical Engineering* **28**, 128–141 (1981).
- [2] Alvarez, R. E. and Macovski, A., "Energy-selective reconstructions in x-ray computerised tomography,"

Physics in Medicine and Biology **21**(5), 733 (1976).

- [3] de Castele, E. V., *Model-based approach for Beam Hardening Correction and Resolution Measurements in Microtomography*, PhD thesis, University Antwerpen (2004).
- [4] Krumm, M., Kasperl, S., and Franz, M., “Reducing non-linear artifacts of multi-material objects in industrial 3d computed tomography,” *NDT & E International* **Vol 41, No 4**, pp 242251 (2008).
- [5] Gompel, G. V., Slambrouck, K. V., Defrise, M., Batenburg, K. J., de Mey, J., Sijbers, J., and Nuyts, J., “Iterative correction of beam hardening artifacts in CT,” *Medical Physics* **38**(S1), S36–S49 (2011).
- [6] Herman, G., “Correction for beam hardening in computed tomography,” *Physics in Medicine and Biology* **24**, 81 (1979).
- [7] Gao, H., Zhang, L., Chen, Z., Xing, Y., and Li, S., “Beam hardening correction for middle-energy industrial computerized tomography,” *Nuclear Science, IEEE Transactions on* **53**(5), 27962807 (2006).
- [8] Shechter, G., Köhler, T., Altman, A., and Proksa, R., “The frequency split method for helical cone-beam reconstruction,” *Medical Physics* **31**(8), 2230–2236 (2004).
- [9] Gao, H., Zhu, L., and Fahrig, R., “Modulator design for x-ray scatter correction using primary modulation: Material selection,” *Medical Physics* **37**(8), 4029–4037 (2010).
- [10] Meyer, E., Raupach, R., Lell, M., Schmidt, B., and Kachelrieß, M., “Frequency split metal artifact reduction (FSMAR) in computed tomography,” *Medical Physics* **39**(4), 1904–1916 (2012).
- [11] Yang, Q., Scherl, H., and Elter, M., “Accelerated quantitative multi-material beam hardening correction(BHC) in cone-beam CT.” European Congress of Radiology (ECR) (2012). DOI: 10.1594/ecr2012/C-2161.
- [12] <http://www.imp.uni-erlangen.de/phantoms/hip/hipphantom.html>.